J. Fluid Mech. (1993), *vol.* 255, *pp.* 275–299

Stochastic characteristics of orbital velocities of random water waves

By WITOLD CIEŚLIKIEWICZ[1] AND OVE T. GUDMESTAD[2]

[1] Institute of Hydroengineering, Polish Academy of Sciences, Kościerska 7, 80-953 Gdańsk, Poland

[2] Statoil, PO Box 300 Forus, 4001 Stavanger, Norway

(Received 5 February 1992 and in revised form 11 January 1993)

This paper presents the stochastic properties of orbital velocities of random water waves in intermediate water depth. Both the emergence effect and weak nonlinear effects are studied; the theoretical predictions are compared with measured kinematics and the deviations from linear theory are quantified.

This study includes new ideas in fluid dynamics. An analytic formula for probability distribution for velocities modified by the emergence effect as well as by nonlinearities of the wave motion in intermediate water depth is developed. This probability function gives us the first statistical moment, the second statistical moment for modified velocities in an *analytical form*, and by numerical integration the third statistical moment for modified velocities.

The theoretical formulae for the statistical moments for surface elevation and for velocities up to third order, with nonlinearities of the motion taken into account, for the case when the emergence effect can be neglected, i.e. below the surface layer, have been developed. This includes a generalized formula for free-surface elevation setdown and calculation of the asymmetry of the horizontal velocity, which is found to be negative in agreement with measurements of Anastasiou *et al.* (1982*b*).

From the first statistical moment of the modified horizontal velocity, the mean flux between any two levels in the wave flume may be calculated. When the integration is carried out from the bottom up to $+\infty$, it leads in approximation to the formula for total mean flux found by Phillips (1960). This agreement with Phillips' formula encourages one to interpret the positive mean value of horizontal velocities as a 'real current'. This interpretation also provides a new understanding of the fluid dynamic implications of results presented by Tung (1975).

Theoretical prediction of the measured kinematics has allowed a better estimation of the return flow in the wave flume, and in the vicinity of the mean water level currents in two different directions are noted. Firstly, the emergence effect gives rise to a current at the mean water level in the direction of the wave advance. Secondly, a flow in the opposite direction, interpreted as a return current in the wave flume, is noticed just below that level.

1. Introduction

For many applications in coastal and offshore engineering, it is necessary to know the water wave kinematics under the waves (Tørum & Gudmestad 1990; Sarpkaya & Isaacson 1981). Normally a random offshore wave field is characterized by a sum of sinusoidal waves with individual energies given by the wave spectrum; however, the

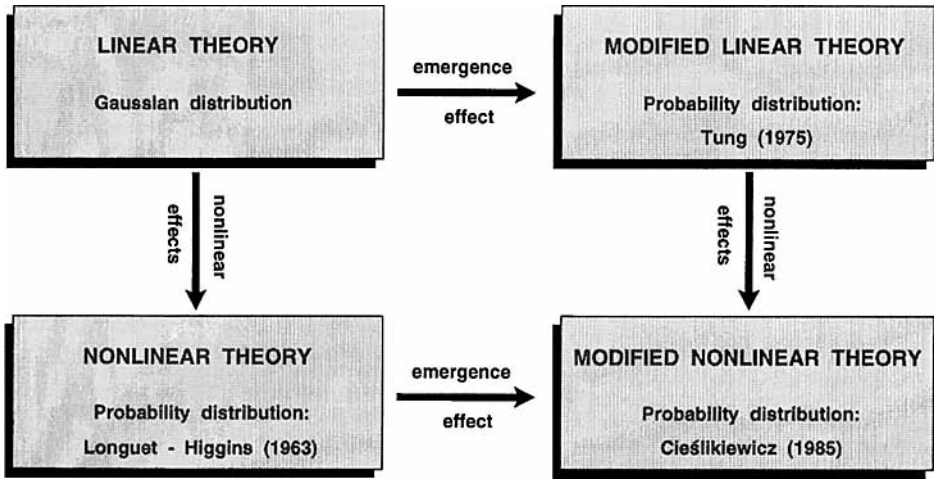

FIGURE 1. Background for the study.

principal shortcoming of linear wave theory for irregular water waves is its inappropriateness in determining kinematic and dynamic parameters near the still water level.

Although some improved methods have been proposed for predicting kinematics in the vicinity of the water surface such as those of Wheeler (1970) and Gudmestad (1990), it should be noted that these represent extrapolations of linear theory and do not satisfy the Laplace equation for fluid flow.

Another reason for deviation from linear theory is that the free surface fluctuates with time, such that a point fixed in space in the vicinity of the mean water level is not submerged at all times but emerges from the water in some phases of the wavy motion. This makes the probability distributions and the corresponding spectral densities different from those of continuously submerged points. This *emergence effect* (Cieślikiewicz 1985; Cieślikiewicz & Massel 1988), as it shall be referred to in this study, is also known as the *free surface fluctuations phenomenon* (Pajouhi & Tung 1975) and has been taken into account in this study following the approach of Tung (1975). This wave theory with the intermittency of submergence taken into account is, furthermore, referred to in the papers of Anastasiou, Tickell & Chaplin (1982*a*, *b*) and Isaacson & Baldwin (1990) as the *intermittent random wave theory*.

The influence of the emergence effect is essential when determining the stochastic characteristics of particle kinematics near the mean water level. The difference between properties when taking into account the emergence effect and when ignoring it decreases considerably for points far from the free surface. On the other hand, it is well known that wave energy is concentrated in the vicinity of the still water level. Thus, the hydrodynamics in this layer is of considerable importance and should therefore be determined with a high degree of accuracy.

Laboratory and field measurements of wave kinematics with emphasis given to the mean water level zone have been reported by Anastasiou *et al.* (1982*a*, *b*) and by Skjelbreia *et al.* (1989, 1991). These latter measurements will be used to demonstrate that the emergence effect modifies the statistics of linear wave theory near the mean water level according to theoretical predictions.

In addition to the emergence effect on the statistics of wave particle kinematics, the influence of nonlinearity of the motion itself will be discussed in a form similar to that of Longuet-Higgins (1963). The background for this study is presented in figure 1.

2. Theory

2.1. *Theoretical development*

In this section the formulae for the probability density and for first two statistical moments of particle velocities will be derived.

Let us consider the orbital velocities $\boldsymbol{u}(\boldsymbol{x}, z, t)$, where $\boldsymbol{x} = [x_1, x_2]$ is the location vector on the horizontal plane, the z-axis is directed vertically upwards and t is the time. It should be pointed out that the non-random parameter z of this random field is chosen from the interval $[-h, \zeta]$, where the upper limit ζ (the free surface of the wave) for a given $\boldsymbol{x}$ and t is a random variable (h is the water depth). This means in fact that $\boldsymbol{u}(\boldsymbol{x}, z, t)$ is not in agreement with the definition of a random field. In order to treat velocity as a random field it can be said that for points above the free surface, the velocity is equal to zero with the probability equal to one. This is not obvious from a 'philosophical' point of view because it is difficult to speak about zero velocity if there is no object (i.e. no water particles in this case) for which the velocity is measured. But this is consistent in an experimental sense since when the point under consideration is above the free surface, the velocimeter will give a zero value.

Let us then for the random process $Y(z)$, where $z \in (-\infty, X]$, introduce the modified random process $\bar{Y}(z)$ for $z \in R^1$ by following the approach of Tung (1975) such that

$$\bar{Y}(z) = \begin{cases} Y(z) & \text{for} \quad z \leqslant X \\ 0 & \text{for} \quad z > X, \end{cases} \tag{1}$$

where X is a random variable.

The modified velocities of a wave field can be now defined:

$$\bar{\boldsymbol{u}}(\boldsymbol{x}, z, t) = \begin{cases} \boldsymbol{u}(\boldsymbol{x}, z, t) & \text{for} \quad z \leqslant \zeta(\boldsymbol{x}, t) \\ \boldsymbol{0} & \text{for} \quad z > \zeta(\boldsymbol{x}, t), \end{cases} \tag{2}$$

in which $\boldsymbol{u} = [u_1, u_2, u_3]$ and $\bar{\boldsymbol{u}} = [\bar{u}_1, \bar{u}_2, \bar{u}_3]$ are the vectors of unmodified and modified water wave orbital velocities, respectively.

It is assumed that $\zeta(\boldsymbol{x}, t)$, $\boldsymbol{u}(\boldsymbol{x}, z, t)$ and $\bar{\boldsymbol{u}}(\boldsymbol{x}, z, t)$ are stationary in time and homogeneous with respect to $\boldsymbol{x}$. Thus, the results obtained for the random variable X and processes Y and $\bar{Y}$ may be applied directly to the free-surface elevations ζ and components of $\boldsymbol{u}$ and $\bar{\boldsymbol{u}}$, owing to the analogous form of (1) and (2).

If the nonlinearity of the wave motion is taken into account, the random field of the free-surface elevation may be presented, after Longuet-Higgins (1963), by the following formula:

$$\zeta(\boldsymbol{x}, t) = \sum_{i=1}^{N} \alpha_i(\boldsymbol{x}, t)\, \xi_i + \sum_{i,j=1}^{N} \alpha_{ij}(\boldsymbol{x}, t)\, \xi_i \xi_j + \sum_{i,j,k=1}^{N} \alpha_{ijk}(\boldsymbol{x}, t)\, \xi_i \xi_j \xi_k + \ldots, \tag{3}$$

where $\alpha_i(\boldsymbol{x}, t), \alpha_{ij}(\boldsymbol{x}, t) \ldots$ are non-random functions, while ξ_i are random variables, assumed to be independent and symmetrically distributed about zero. It is suggested that a similar representation may be used for the nonlinear random process Y:

$$Y(z) = \sum_{i=1}^{N} \beta_i(z)\, \xi_i + \sum_{i,j-1}^{N} \beta_{ij}(z)\, \xi_i \xi_j + \sum_{i,j,k=1}^{N} \beta_{ijk}(z)\, \xi_i \xi_j \xi_k + \ldots, \tag{4}$$

where, as before, the functions $\beta_i(z), \beta_{ij}(z) \ldots$ are not random. For the variable X it is assumed that there exists a representation analogous to (3):

$$X = \sum_{i=1}^{N} \alpha_i\, \xi_i + \sum_{i,j=1}^{N} \alpha_{ij}\, \xi_i \xi_j + \sum_{i,j,k=1}^{N} \alpha_{ijk}\, \xi_i \xi_j \xi_k + \ldots, \tag{5}$$

where $\alpha_i, \alpha_{ij} \ldots$ are non-random constants.

The probability densities for X and Y, $f_X(x)$ and $f_Y(y;z)$, respectively, may be found by following Longuet-Higgins (1963). Introducing

$$Z(\gamma) = \frac{1}{(2\pi)^{\frac{1}{2}}} e^{-\gamma^2/2} \tag{6}$$

the second-order approximation is

$$f_X(x) = \frac{1}{\sigma_X} Z(x') [1 + \tfrac{1}{6}\lambda_{30} H_3(x')], \tag{7}$$

$$f_Y(y;z) = \frac{1}{\sigma_Y(z)} Z(y') [1 + \tfrac{1}{6}\lambda_{03}(z) H_3(y')], \tag{8}$$

where

$$\left.\begin{aligned} \lambda_{mn} &= \frac{\mu_{mn}}{(\mu_{20}^m \mu_{02}^n)^{\frac{1}{2}}}, \\ x' &= \frac{x - m_{10}}{\sigma_X}, \quad y' = \frac{y - m_{01}}{\sigma_Y}. \end{aligned}\right\} \tag{9}$$

Note that m_{10}, σ_X, λ_{30} are constants while m_{01}, σ_Y, λ_{03} are functions of z. μ_{mn} are the central joint moments for X and Y given as

$$\mu_{mn} = \langle (X - \langle X \rangle)^m (Y - \langle Y \rangle)^n \rangle, \tag{10}$$

where $\langle \cdot \rangle$ is the expected value of a quantity enclosed in the angle brackets, and $m_{10} = \langle X \rangle$, $m_{01} = \langle Y \rangle$, $\sigma_X = \mu_{20}^{\frac{1}{2}}$, $\sigma_Y = \mu_{02}^{\frac{1}{2}}$.

In (7) and (8) $H_3(\cdot)$ denotes a Hermite polynomial of the third degree. Note that for the calculation of Hermite polynomials of the nth degree, the following relation is used:

$$(-1)^m \frac{\partial^m}{\partial x^m} e^{-x^2/2} = H_m(x) e^{-x^2/2}, \tag{11}$$

in which it is assumed that $\partial^0/\partial x^0$ is a neutral operator.

The probability that the random variable X exceeds the value z is equal to

$$P[X \geqslant z] = \int_z^\infty f_X(x)\, dx = Q^*(z'). \tag{12}$$

Here $z' = (z - m_{10})/\sigma_X$ and

$$Q^*(\gamma) = Q(\gamma) + \tfrac{1}{6}\lambda_{30} H_2(\gamma) Z(\gamma), \tag{13}$$

in which

$$Q(\gamma) = \int_\gamma^\infty Z(z)\, dz. \tag{14}$$

Cieślikiewicz (1985) obtained the following formula describing the probability density of the modified process $\bar{Y}(z)$ (see Appendix A):

$$f_{\bar{Y}}(y;z) = [1 - Q^*(z')]\, \delta(y) + \frac{1}{\sigma_Y(z)} Z(y') \times \left\{ [1 + \tfrac{1}{6}\lambda_{03}(z) H_3(y')]\, Q[\eta(z', y'; r)] + \frac{1}{6\Delta^{\frac{1}{2}}} G(y', z')\, Z[\eta(z', y'; r)] \right\}, \tag{15}$$

where $r = \lambda_{11}(z)$ is the coefficient of cross-correlation between X and Y; $\delta(\cdot)$ denotes the Dirac's δ-function and $\eta(z', y'; r) = (z' - ry')/\Delta^{\frac{1}{2}}$ in which $\Delta = 1 - r^2$. The function G in (15) is

$$G(y', z') = \lambda_{30} H_{20}(z', y'; r) + 3\lambda_{21} H_{11}(z', y'; r) + 3\lambda_{12} H_{02}(z', y'; r)$$
$$- \lambda_{03} \frac{r}{\Delta} \{r^2 H_2[\eta(z', y'; r)] - 3\Delta^{\frac{1}{2}} r H_1[\eta(z', y'; r)] H_1(y') + 3\Delta H_2(y')\}. \quad (16)$$

Two-dimensional equivalents of the Hermite polynomials appearing in (16) may be calculated using the relation

$$(-1)^{m+n} \frac{\partial^m}{\partial x^m} \frac{\partial^n}{\partial y^n} e^{-[y^2+\eta^2(x, y; r)]/2} = H_{mn}(x, y; r) e^{-[y^2+\eta^2(x, y; r)]/2}. \quad (17)$$

Note that (15) represents an extension of (8) by including emergence effects (figure 1).

Anastasiou *et al.* (1982*b*) have also calculated the probability distribution for particle velocity taking into account both the emergence effect and weak nonlinearities, but they obtained the final results by numerical integration. Moreover, the parameters of the probability distribution which are discussed in the next paragraphs, were obtained differently.

The mean value and the second moment calculated by using (15) may be written as (for details see Appendix A)

$$\langle \bar{Y} \rangle = m_{01} Q^*(z') + \sigma_Y Z(z') [r + \tfrac{1}{6}(r\lambda_{30} H_3(z') + 3\lambda_{21} H_1(z'))], \quad (18)$$
$$\langle \bar{Y}^2 \rangle = (\sigma_Y^2 + m_{01}^2) Q^*(z') + \sigma_Y^2 Z(z') (r^2 H_1(z') + \tfrac{1}{6}\lambda_{30} H_4(z') + r\lambda_{21} H_2(z') + \lambda_{12})$$
$$+ 2m_{01} \sigma_Y Z(z') [r + \tfrac{1}{6}(r\lambda_{30} H_3(z') + 3\lambda_{21} H_1(z'))], \quad (19)$$

and the variance $\sigma_{\bar{Y}}^2(z)$ can be calculated using the formula

$$\sigma_{\bar{Y}}^2(z) = \langle \bar{Y}^2 \rangle - \langle \bar{Y} \rangle^2. \quad (20)$$

In (15) terms including λ_{mn} for $m+n = 3$ represent nonlinear effects. If one omits these effects, the probability density given by (15) will take a simpler form, as given by Tung (1975):

$$f_Y(y; z) = [1 - Q(z')] \delta(y) + \frac{1}{\sigma_Y(z)} Z(y') Q[\eta(z', y'; r)], \quad (21)$$

where $y' = y/\sigma_Y$. Equation (21) represents the emergence effect in (15) (figure 1). Similarly, for the moments $\langle \bar{Y} \rangle$ and $\langle \bar{Y}^2 \rangle$ we obtain

$$\langle \bar{Y} \rangle = r\sigma_Y Z(z'), \quad (22)$$
$$\langle \bar{Y}^2 \rangle = \sigma_Y^2 Q(z') + \sigma_Y^2 r^2 z' Z(z'). \quad (23)$$

It can be shown easily that with $z \to -\infty$ the probability density for process $\bar{Y}$ given by (15) becomes equal to the density for the process Y as given by (8). From (18), (19) and (20) it follows that:

$$\lim_{z \to -\infty} \langle \bar{Y} \rangle = m_{01}, \quad \lim_{z \to -\infty} \langle \bar{Y}^2 \rangle = \sigma_Y^2 + m_{01}^2, \quad \lim_{z \to -\infty} \sigma_{\bar{Y}}^2 = \sigma_Y^2. \quad (24)$$

Thus the emergence effect ceases to be of significance for points located deeply below the free surface.

2.2. *Parameters of the probability distribution for a wave field*

In order to calculate the quantities m_{10}, σ_X and λ_{30} appearing in (7) and (9) (remember that X and Y play to the role of surface elevation ζ and velocity component in a wave field, respectively), the central statistical moments μ_{20} and μ_{30} for surface elevation

should be known. Starting from the basic hydrodynamic equation for fluid flow, i.e. the Laplace equation, and the nonlinear boundary conditions at the free surface, these statistical parameters can be calculated based on the free-surface spectral density.

If the linear part of the spectrum is denoted by $F^{(1)}(\boldsymbol{k})$ (Appendix B), where $\boldsymbol{k}$ is the wavenumber vector, then following relations hold (Cieślikiewicz 1989):

$$m_{10} = \frac{1}{2}\int_{\boldsymbol{k}} \tilde{k}(1-\tanh^{-2}kh)\,F^{(1)}(\boldsymbol{k})\,\mathrm{d}\boldsymbol{k}, \tag{25}$$

$$\mu_{20} = \int_{\boldsymbol{k}} F^{(1)}(\boldsymbol{k})\,\mathrm{d}\boldsymbol{k}, \tag{26}$$

and

$$\mu_{30} = \int_{\boldsymbol{k}}\int_{\boldsymbol{k}'} K_{30}(\boldsymbol{k},\boldsymbol{k}')\,F^{(1)}(\boldsymbol{k})\,F^{(1)}(\boldsymbol{k}')\,\mathrm{d}\boldsymbol{k}\,\mathrm{d}\boldsymbol{k}', \tag{27}$$

where

$$K_{30}(\boldsymbol{k},\boldsymbol{k}') = \frac{3}{(\tilde{k}\tilde{k}')^{\frac{1}{2}}}B(\boldsymbol{k},\boldsymbol{k}'), \tag{28}$$

$$B(\boldsymbol{k},\boldsymbol{k}') = B^{-}(\boldsymbol{k},\boldsymbol{k}') + B^{+}(\boldsymbol{k},\boldsymbol{k}') - \boldsymbol{k}\cdot\boldsymbol{k}' + (\tilde{k}+\tilde{k}')(\tilde{k}\tilde{k}')^{\frac{1}{2}}, \tag{29}$$

$$B^{\pm}(\boldsymbol{k},\boldsymbol{k}') = \frac{(\tilde{k}^{\frac{1}{2}}\pm\tilde{k}'^{\frac{1}{2}})^2(\boldsymbol{k}\cdot\boldsymbol{k}'\mp\tilde{k}\tilde{k}') + (\tilde{k}^{\frac{1}{2}}\pm\tilde{k}'^{\frac{1}{2}})(\tilde{k}'^{\frac{1}{2}}R\pm\tilde{k}^{\frac{1}{2}}R')}{(\tilde{k}^{\frac{1}{2}}\pm\tilde{k}'^{\frac{1}{2}})^2 - |\boldsymbol{k}\pm\boldsymbol{k}'|\tanh|\boldsymbol{k}\pm\boldsymbol{k}'|h}. \tag{30}$$

In these formulae

$$R = \tfrac{1}{2}(k^2-\tilde{k}^2), \quad R' = \tfrac{1}{2}(k'^2-\tilde{k}'^2), \tag{31}$$

and

$$\tilde{k} = |\boldsymbol{k}|\tanh|\boldsymbol{k}|h, \quad \tilde{k}' = |\boldsymbol{k}'|\tanh|\boldsymbol{k}'|h. \tag{32}$$

Expression (25) for the mean water level in the case of an idealized narrow spectrum $F^{(1)}(\boldsymbol{k}) = \sigma_0^2\,\delta(\boldsymbol{k}-\boldsymbol{k}_0)$ gives $\langle\zeta\rangle = -\sigma_0^2 k_0/\sinh 2k_0 h$ in which $k_0 = |\boldsymbol{k}_0|$. If a is a slowly changing random wave amplitude, we obtain the well-known formula for mean water level setdown $\langle\zeta\rangle = -\frac{1}{2}\langle a^2\rangle k_0/\sinh 2k_0 h$. It can be noted, that for deep water, with $h\to\infty$ the mean value of free-surface elevation tends to zero:

$$\lim_{h\to\infty} m_{10} = 0. \tag{33}$$

In order to determine the parameters of the probability function as given by (15) for modified velocities, the statistical moments for unmodified velocity quantities ought to be calculated together with the joint moments for them and ζ, up to third order inclusive. The relevant formulae can be found in Cieślikiewicz (1989). These are as follows:

$$m_{01}^{u_\nu} = 0 \quad \text{for} \quad \nu = 1,2,3, \tag{34}$$

$$\mu_{02}^{u_\nu} = g\int_{\boldsymbol{k}} \frac{k_\nu^2}{\tilde{k}}\frac{\cosh 2k(z+h)+1}{\cosh 2kh+1}F^{(1)}(\boldsymbol{k})\,\mathrm{d}\boldsymbol{k}, \quad \nu = 1,2, \tag{35}$$

$$\mu_{02}^{u_3} = g\int_{\boldsymbol{k}} \tilde{k}\frac{\cosh 2k(z+h)-1}{\cosh 2kh-1}F^{(1)}(\boldsymbol{k})\,\mathrm{d}\boldsymbol{k}, \tag{36}$$

$$\mu_{11}^{u_\nu} = \int_{\boldsymbol{k}} \left(\frac{g}{\tilde{k}}\right)^{\frac{1}{2}} k_\nu \frac{\cosh k(z+h)}{\cosh kh}F^{(1)}(\boldsymbol{k})\,\mathrm{d}\boldsymbol{k}, \quad \nu = 1,2, \tag{37}$$

$$\mu_{11}^{u_3} = 0. \tag{38}$$

For the statistical moments of third order we can write

$$\mu_{mn}^{u_\nu} = \int_{\boldsymbol{k}}\int_{\boldsymbol{k}'} K_{mn}^{u_\nu}(\boldsymbol{k},\boldsymbol{k}';z)\,F^{(1)}(\boldsymbol{k})\,F^{(1)}(\boldsymbol{k}')\,\mathrm{d}\boldsymbol{k}\,\mathrm{d}\boldsymbol{k}', \tag{39}$$

where $m, n = 0, \ldots, 3$ and $m+n = 3$, and where functions $K^{u_\nu}_{mn}$ can be written in the following form:

$$K^{u_\nu}_{03}(\boldsymbol{k}, \boldsymbol{k}'; z) = 3g\, g^{\frac{1}{2}} \frac{k_\nu k'_\nu}{\tilde{k}\tilde{k}'} [(k_\nu - k'_\nu)\, C^-(\boldsymbol{k}, \boldsymbol{k}'; z)$$

$$+ (k_\nu + k'_\nu)\, C^+(\boldsymbol{k}, \boldsymbol{k}'; z)] \frac{\cosh k(z+h) \cosh k'(z+h)}{\cosh kh \cosh k'h} \quad \text{for} \quad \nu = 1, 2, \tag{40}$$

in which $\boldsymbol{k} = [k_1, k_2]$ and

$$C^\pm(\boldsymbol{k}, \boldsymbol{k}'; z) = \frac{B^\pm(\boldsymbol{k}, \boldsymbol{k}')}{\tilde{k}^{\frac{1}{2}} \pm \tilde{k}'^{\frac{1}{2}}} \frac{\cosh k^\pm(z+h)}{\cosh k^\pm h} \tag{41}$$

and

$$k^\pm = |\boldsymbol{k}^\pm| = |\boldsymbol{k} \pm \boldsymbol{k}'|. \tag{42}$$

Next

$$K^{u_3}_{03} = 0, \tag{43}$$

$$K^{u_\nu}_{21}(\boldsymbol{k}, \boldsymbol{k}'; z) = \left(\frac{g}{\tilde{k}\tilde{k}'}\right)^{\frac{1}{2}} \left\{ (k_\nu - k'_\nu)\, C^-(\boldsymbol{k}, \boldsymbol{k}'; z) \right.$$

$$\left. + (k_\nu + k'_\nu)\, C^+(\boldsymbol{k}, \boldsymbol{k}'; z) + \frac{2k'_\nu}{\tilde{k}'^{\frac{1}{2}}} B(\boldsymbol{k}, \boldsymbol{k}') \frac{\cosh k'(z+h)}{\cosh k'h} \right\} \quad \text{for} \quad \nu = 1, 2, \tag{44}$$

$$K^{u_3}_{21} = 0, \tag{45}$$

$$K^{u_\nu}_{12}(\boldsymbol{k}, \boldsymbol{k}'; z) = \frac{g k'_\nu}{\tilde{k}' \tilde{k}^{\frac{1}{2}}} \frac{\cosh k'(z+h)}{\cosh k'h} \left\{ \frac{k_\nu}{\tilde{k}^{\frac{1}{2}}} B(\boldsymbol{k}, \boldsymbol{k}') \frac{\cosh k(z+h)}{\cosh kh} \right.$$

$$\left. + 2[(k_\nu - k'_\nu)\, C^-(\boldsymbol{k}, \boldsymbol{k}'; z) + (k_\nu + k'_\nu)\, C^+(\boldsymbol{k}, \boldsymbol{k}'; z)] \right\} \quad \text{for} \quad \nu = 1, 2, \tag{46}$$

$$K^{u_3}_{12}(\boldsymbol{k}, \boldsymbol{k}'; z) = g \frac{\sinh k'(z+h)}{\sinh k'h} \left\{ [B^-(\boldsymbol{k}, \boldsymbol{k}') - B^+(\boldsymbol{k}, \boldsymbol{k}') - \tilde{k}\tilde{k}'] \frac{\sinh k(z+h)}{\sinh kh} \right.$$

$$\left. - \frac{2}{\tilde{k}^{\frac{1}{2}}} [|\boldsymbol{k} - \boldsymbol{k}'| \tanh |\boldsymbol{k} - \boldsymbol{k}'|\, hD^-(\boldsymbol{k}, \boldsymbol{k}'; z) - |\boldsymbol{k} + \boldsymbol{k}'| \tanh |\boldsymbol{k} + \boldsymbol{k}'|\, hD^+(\boldsymbol{k}, \boldsymbol{k}'; z)] \right\}, \tag{47}$$

where functions D^+ and D^- are defined as follows:

$$D^\pm(\boldsymbol{k}, \boldsymbol{k}'; z) = C^\pm(\boldsymbol{k}, \boldsymbol{k}'; z) \frac{\cosh k^\pm(z+h)}{\cosh k^\pm h}. \tag{48}$$

It can be seen from the above formulae that the weak nonlinearities (within the frame of the adopted approximation) do not affect the mean values $m^{u_\nu}_{01}$ of particle velocities, which remain equal to zero (see (34)). Variances $\mu^{u_\nu}_{02}$ given by (35) and (36) of the orbital velocities are left unchanged (see also Appendix B). However, the nonlinearity of the motion leads to non-zero skewness for the horizontal velocity (see $\mu^{u_\nu}_{03}$ for $\nu = 1, 2$ given by (39) and (40)). Skewness of the vertical component still remains equal to zero (see $\mu^{u_3}_{03}$ given by (39) and (45)).

The influence of the emergence effect on the orbital velocities, as given in (2), however, leads to a modification of the probability density for the velocity from that expressed by (8) to the form given by (15). It also results in a non-zero mean value given by (18) for the horizontal velocities and in modified variances (20) for both horizontal and vertical velocity components. It should be noted from (18) that the mean value of the vertical component remains equal to zero in view of (38) and (45).

The above analysis yields the conclusion that the effectiveness and accuracy of the evaluation of statistical properties of velocities depends very strongly on the spectral density function of surface elevation. Therefore, in the following analysis of data, the spectral analysis will be described in some detail.

2.3. *Total mean flux*

Now, let us consider in the first-order approximation (i.e. when λ_{mn} for $m+n=3$ are neglected) the total mean flux $\boldsymbol{q}=[q_1, q_2]$ with components defined as

$$q_\nu = \int_{-h}^{\infty} \langle \bar{u}_\nu(z) \rangle \, \mathrm{d}z \quad \text{for} \quad \nu = 1,2. \tag{49}$$

By using (22) and (37) the above integrals may be rewritten as follows:

$$\begin{aligned} q_\nu &= \frac{1}{\sigma_\zeta} \int_{-h}^{\infty} Z(z') \left[\int_{\boldsymbol{k}} \left(\frac{g}{\tilde{k}}\right)^{\frac{1}{2}} k_\nu \frac{\cosh k(z+h)}{\cosh kh} F^{(1)}(\boldsymbol{k}) \, \mathrm{d}\boldsymbol{k} \right] \mathrm{d}z \\ &= \frac{1}{\sigma_\zeta} \int_{\boldsymbol{k}} \left(\frac{g}{\tilde{k}}\right)^{\frac{1}{2}} \frac{k_\nu}{\cosh kh} F^{(1)}(\boldsymbol{k}) \left[\int_{-h}^{\infty} \cosh k(z+h) \, Z(z') \, \mathrm{d}z \right] \mathrm{d}\boldsymbol{k} \quad \text{for} \quad \nu = 1,2, \end{aligned} \tag{50}$$

in which $\sigma_\zeta = \mu_{20}^{\frac{1}{2}}$ is the standard deviation of the surface elevation ζ. The integration over z can be performed without difficulty, resulting in the following form of the total mean flux q_ν:

$$q_\nu = \int_{\boldsymbol{k}} \left(\frac{g}{\tilde{k}}\right)^{\frac{1}{2}} \frac{k_\nu}{\cosh kh} W(-h; \sigma_\zeta, k) \, F^{(1)}(\boldsymbol{k}) \, \mathrm{d}\boldsymbol{k}, \tag{51}$$

where the function W is defined as

$$\begin{aligned} W(z_a; \sigma, k) &= \int_{z_a/\sigma}^{\infty} \cosh k(z+h) \, Z(z) \, \mathrm{d}z \\ &= \tfrac{1}{2} \mathrm{e}^{\sigma^2 k^2/2} \{ \mathrm{e}^{kh} Q(z_a/\sigma + k\sigma) + \mathrm{e}^{-kh} Q(z_a/\sigma - k\sigma) \}. \end{aligned} \tag{52}$$

The more general form of the function

$$W(z_a, z_b; \sigma, k) = \int_{z_a/\sigma}^{z_b/\sigma} \cosh k(z+h) \, Z(z) \, \mathrm{d}z$$

can be found in Cieślikiewicz & Massel (1988) and may be used if one needs to calculate the flux between elevations z_a and z_b.

If we take polar coordinates (k, θ) in the $\boldsymbol{k}$-plane, we can introduce the directional spectrum $\hat{F}(\omega, \theta)$ by

$$F(\boldsymbol{k}) \, \mathrm{d}\boldsymbol{k} = F(k, \theta) \, k \, \mathrm{d}k \, \mathrm{d}\theta = \hat{F}(\omega, \theta) \, \mathrm{d}\omega \, \mathrm{d}\theta \tag{53}$$

and the dispersion relation

$$\omega^2(k) = gk \tanh kh. \tag{54}$$

In the one-directional case, when $\hat{F}(\omega, \theta)$ vanishes everywhere except for $\theta = \theta_0$, we have from (51)

$$q = \int_0^{\infty} \frac{gk}{\omega \cosh kh} W(-h; \sigma_\zeta, k) \, S^{(1)}(\omega) \, \mathrm{d}\omega, \tag{55}$$

where

$$S^{(1)}(\omega) = \int_{-\pi}^{\pi} \hat{F}^{(1)}(\omega, \theta) \, \mathrm{d}\omega \, \mathrm{d}\theta$$

denotes the linear part of the frequency spectrum

$$S(\omega) = \int_{-\pi}^{\pi} \hat{F}(\omega, \theta)\, \mathrm{d}\omega\, \mathrm{d}\theta.$$

In the integral (55) the wavenumber k is related to the angular frequency ω by the dispersion relation (54).

In the assumed approximation, the difference between $S(\omega)$ and $S^{(1)}(\omega)$ can be neglected (see Appendix B). Assuming further that

(i) $k_p \sigma_\zeta \ll 1$ (where k_p is the wavenumber corresponding to the peak frequency) and that the spectrum $S(\omega)$ decays quickly enough for $\omega \to \infty$;

(ii) the water depth h is large enough (in practice it is sufficient to have $h > 3\sigma_\zeta$), in (55) one can set $Q(-h' \pm k\sigma_\zeta) \approx 1$ ($h' = h/\sigma_\zeta$). Thus, the total mean flux obtains the following approximate form:

$$q \approx \int_0^\infty \frac{gk}{\omega} \exp\left[\tfrac{1}{2}\sigma_\zeta^2 k^2\right] S(\omega)\, \mathrm{d}\omega. \tag{56}$$

Note that the above expression is accurate for infinite water depth $h \to \infty$. Because it is assumed that $\sigma_\zeta k$ has a small value for k such that the corresponding ω (through the dispersion relation (54)) gives a value of $S(\omega)$ that is not infinitely small, we can find an even simpler form of (56). Expanding $\exp(\cdot)$ into Taylor series gives

$$\exp\left[\tfrac{1}{2}\sigma_\zeta^2 k^2\right] = 1 + \tfrac{1}{4}\sigma_\zeta^2 k^2 + \ldots \approx 1; \tag{57}$$

thus

$$q \approx \int_0^\infty \frac{gk}{\omega} S(\omega)\, \mathrm{d}\omega, \tag{58}$$

which is a result obtained by Phillips (1960).

Note that, by (37), the approximate total mean flux (58) can be written as

$$q \approx \mu_{11}^u|_{z=0} = \langle \zeta u(x, 0, t) \rangle, \tag{59}$$

which is of a form analogous to that for the case of deterministic small-amplitude waves $q \approx \overline{\zeta u(x, 0, t)}$ (see Phillips 1977), where bar denotes the mean value over a wave period.

For deep water waves (58) can be rewritten as $q = \int_0^\infty \omega S(\omega)\, \mathrm{d}\omega$ which is the value of the spectral moment of the first order m_1.

3. Experiment

3.1. *Experimental set-up*

The experimental arrangement and subsequent results discussed below are described in detail in papers by Skjelbreia *et al.* (1989, 1991). The experiments were carried out in a tank 33 m long, 1.02 m wide and 1.8 m deep. The irregular wave generator of this tank is hydraulically driven and the control signal was constructed from a JONSWAP target wave spectrum using JONSWAP peakedness factor $\gamma = 3.0$, allowing for no periodicity in the free-surface signal.

At the end of the tank, opposite the wave generator, was located a passive wave absorber consisting of a series of vertical perforated steel plates. The reflection coefficient was estimated as $\approx 5\%$ over a broad frequency range.

The surface elevation for each wave case studied by Skjelbreia *et al.* (1989) was generated from one spectrum and was measured with seven standard resistive-type

Run	Measurement level z (m)	Statistical properties of surface elevation: Mean value (m) ($\times 10^{-3}$)	Standard deviation (m) ($\times 10^{-2}$)	Skewness ($\times 10^{-1}$)	Kurtosis-3 ($\times 10^{-1}$)
30	0.20	−1.69	5.387	2.59	1.78
27	0.15	−2.00	5.488	2.50	1.64
15	0.10	−2.08	5.675	2.65	1.50
10	0.05	−2.17	5.410	2.46	1.66
25	0.00	−1.28	5.334	2.49	1.78
23	−0.05	−1.36	5.464	2.62	1.64
1	−0.10	−1.99	5.340	2.41	2.24
7	−0.20	−2.33	5.395	2.48	1.85
16	−0.25	−1.99	5.645	2.67	1.50
18	−0.50	−4.18	5.361	2.55	1.97
20	−1.00	−3.09	5.335	2.47	2.29
34	−1.105	−2.50	5.293	2.38	2.30

TABLE 1. LDV locations and statistical properties of surface elevation for analysed Case 5 runs.

gauges. The special arrangement of the gauges was adopted to decompose incoming and reflected irregular waves (Zelt & Skjelbreia 1992). Three gauges were placed close to each other in order to resolve the first-order waves, while another four gauges were distributed along wave tank to resolve long waves. The wave gauge positions were accurate to 0.01 m.

The flow velocity was measured on the centreline at a single longitudinal position along the tank, coinciding with one of the gauges, but at several different elevations by a two-component laser-Doppler velocimeter (LDV). The two velocity components were measured in a plane parallel to the sidewall of the tank with a measurement volume cross-section of approximately 100 μm in diameter. The LDV was specifically designed for this study and had the special feature of using only a single laser beam in the flow.

The LDV allowed measurements from a wave crest down to the tank bottom but at one point in space only during one run. In order to obtain the distributions for the statistical properties of the velocity along the vertical axis it was necessary to repeat the experiment with exactly the same free-surface elevation spectrum but locating the LDV station at different vertical positions. Therefore great care was given to maintain reproducible wave conditions in the tank. It was found that it is very important for reproducibility of the wave flow to keep a constant water depth. Special attention was paid to measuring orbital velocity components within the surface layer.

Each run in the test program had a duration of 819.2 s. All seven wave gauge channels were sampled simultaneously with the two LDV channels at a rate of 40 Hz.

3.2. *Statistical analysis of measured free-surface elevation and particle kinematics*

In order to examine the variation of the stochastic properties of velocities with z-elevation for one wave case, the analysis of 12 runs for various LDV locations was carried out. These runs, reproducing the wave conditions in the tank for a selected sea state as given by the significant wave height $H_S = 0.21$ m and the peak period $T_p = 1.8$ s (Skjelbreia *et al.* 1989, 1991, Case 5 – measurement series I18), are listed in table 1.

Digitization of the free-surface elevation and velocity time series was carried at a rate

of 40 Hz and samples of 32768 measuring points were collected. The first 2048 and last 1024 data points for each time series were omitted in order to cancel possible transition effects, giving finally the $N = 29696$ point length sequence.

Measurements of the particle velocity near the mean water level are to varying degrees influenced by the emergence effect depending upon the level at which they were obtained. This occurs when the probe volume of the LDV emerges from the water. Until the water surface moves back up to the level of the LDV the signal holds at the last measured value (Skjelbreia *et al.* 1989). Time series of particle velocities u_i and w_i were therefore modified numerically such that their values during drop-out periods were set equal to zero:

$$[\bar{u}_i, \bar{w}_i] = [u_i, w_i]\,\mathscr{H}(\zeta_i - z), \tag{60}$$

in which z is the level of the LDV and $\mathscr{H}(\cdot)$ is the Heaviside unit step function. In (60), and below in this section, the notation has been changed for convenience. Namely, the subscript indicates the number of data point in the sample, while the velocity components are u, v, w, i.e. $\boldsymbol{u} = [u, v, w]$ and $\bar{\boldsymbol{u}} = [\bar{u}, \bar{v}, \bar{w}]$. Equation (60) is of course in agreement with (2).

The time series ζ_i, $\bar{u}_i$ and $\bar{w}_i$ were subjected to statistical and spectral analysis. The statistical analysis involved calculation of the first four statistical moments, coefficients of skewness and kurtosis and probability density functions for each series. Also, joint statistical moments for surface elevation and orbital velocities were calculated. In this subsection spectral analysis results of the data are presented while those concerning probability distributions will be discussed in the next subsection.

For the spectral calculations segmental smoothing was required. This was done according to the 'Welch method' (Oppenheim & Schafer 1975). The sequences of length $N = 29696$ points were divided into 57 sections of $M = 1024$ points each. The segments were overlapped by one half of their length. Successive sections were multiplied by a Hanning window, transformed with a 1024-point FFT, summed and averaged. This smoothing resulted in a number of degrees of freedom equal to twice the number of sections that the sequence was divided into, i.e. 114. The 95% confidence intervals were estimated by calculating the variance of the unaveraged spectral estimates under the assumption of normal distribution.

The power spectra for 513 frequency values evenly spaced between 0 and the Nyquist frequency ($f_c = 20$ Hz) were obtained. For the wave case analysed the peak frequency $f_p \approx 0.56$ Hz, and for the most energetic range $(0, 3f_p)$ 43 values of the power spectra were obtained with discrete frequency spacing $\Delta f = 0.039$ Hz ($\Delta\omega = 0.245$ rad/s).

The measured spectra of surface elevation were used to calculate the statistical parameters for the particle kinematics (§2). These calculations involve numerical integration over frequency. In order to obtain the integrals with high accuracy and with a small number of function evaluations of the integrand, the adaptive recursive Gaussian quadrature method was used. Cubic spline interpolation was used to prepare function segments suitable for the computer program.

Figure 2 shows the estimated spectral density of surface elevation ζ for Run 1. It is noted that the measured spectrum shows no obvious secondary peak. Cases with higher degrees of nonlinearity were not available from Skjelbreia *et al.*'s series of experiments. It should be noted that very good reproducibility of wave conditions was obtained in the tank – at least when spectral density of the surface elevation is considered. Deeper insight into this question is obtained from examination of the first four statistical moments of the free-surface elevation. In table 1 the mean values, standard deviations, skewness and kurtosis coefficients are presented for the 12 runs of wave case 5 (I18). Skewness is not much greater than 0.2 for each of them, which means

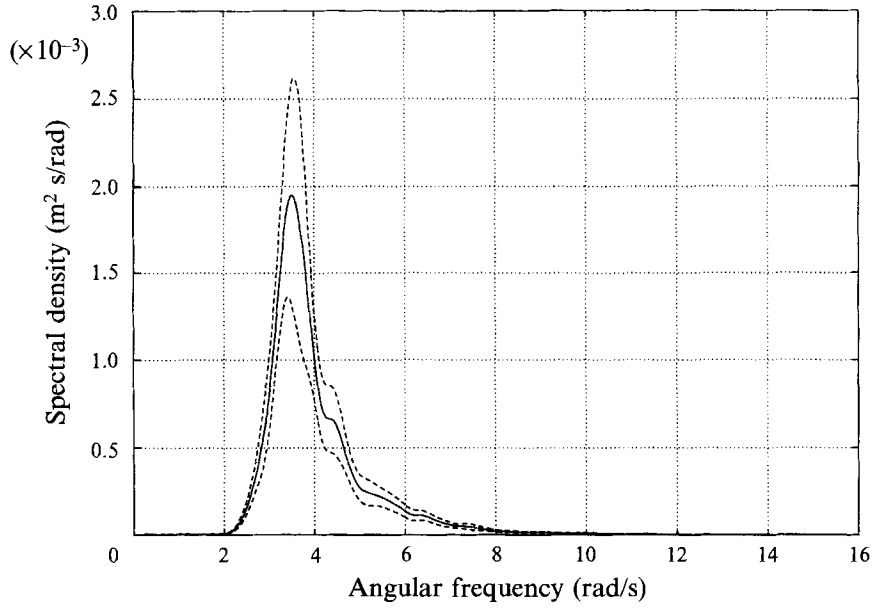

FIGURE 2. Power spectrum of free-surface elevation for Run 1, $z = -0.10$ m; ---, 95% confidence limits.

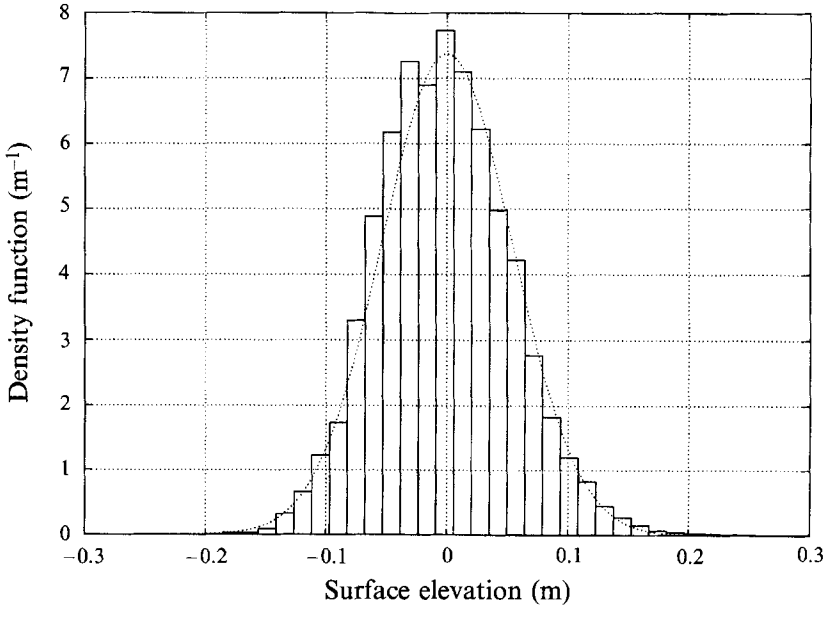

FIGURE 3. Comparison of the observed (bar plot) and Gaussian probability distribution (·····) for the free-surface elevation, Run 10.

that strong deviations from the Gaussian distribution (Ochi & Wang 1984) should not be expected for the free surface.

In figure 3 a histogram with 30 equally spaced bins between the minimum and maximum values of ζ for run 10 is presented, showing the estimated probability

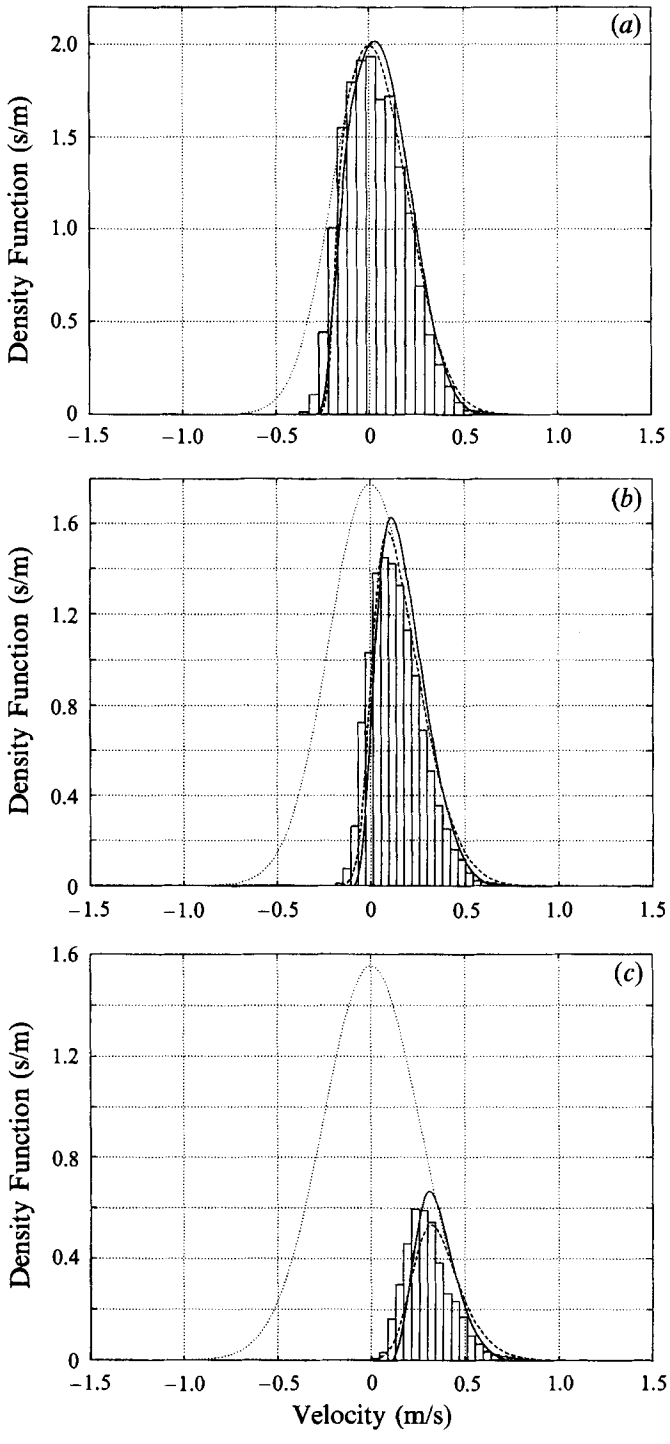

FIGURE 4. Continuous part of probability density function of the horizontal velocity for various z: (*a*) Run 23, $z = -0.05$ m, (*b*) Run 25, $z = 0$ m, (*c*) Run 10, $z = 0.05$ m. Bar plot, observed values; ——, second-order according to (15); – – –, first-order according to (21); · · · · ·, first-order without emergence effect (Gaussian).

distribution of the free-surface elevation. Values of p_i of the histogram are scaled such that direct comparison with the probability density function is possible:

$$p_i = \frac{n_i}{N\Delta_\zeta} \quad \text{for} \quad i = 1, 2, \ldots, 30, \tag{61}$$

in which N is the number of data points (29696 in this example), n_i is the number of data points observed in the ith bin and Δ_ζ is the width of the bin. Outliers greater than 5 standard deviations were removed which gave a bin width of $\Delta_\zeta \leqslant \frac{1}{3}\sigma_\zeta$.

It is seen from figure 3 that measured surface elevations deviate only slightly from the Gaussian distribution. This means that for points that are continuously submerged we should not expect significant deviations from the linear wave theory.

3.3. *Comparison of theoretical and observed probability distributions of velocities*

In order to calculate the probability density function and statistical moments for the velocities, the linear part of the spectral density should be known. In the second-order approximation it can be assumed (Appendix B) that

$$F(\boldsymbol{k}) \approx F^{(1)}(\boldsymbol{k}). \tag{62}$$

This means that the observed spectrum is identified by its linear part. Moreover, a case when all spectral components propagate in one direction only is considered. In the numerical integration the energy contained in the frequency interval $\omega > 3\omega_p$ was neglected, i.e. an upper frequency cutoff was applied. Thus the frequency spectrum was taken as

$$\tilde{S}(\omega) = S(\omega)\,\mathscr{H}(3\omega_p - \omega), \tag{63}$$

in which $S(\omega)$ is the measured spectral density of free elevation.

As the wave is unidirectional, the formulae describing the moments for processes ζ, $\boldsymbol{u}$ (§2) become much simpler. Using a polar coordinate system (k, θ) in the $\boldsymbol{k}$-vector plane, a directional spectrum $\hat{F}(\omega, \theta)$ is introduced satisfying (53). Since the wave is unidirectional, integration over θ may be done immediately, giving

$$S(\omega) = \int_{-\pi}^{\pi} \hat{F}(\omega, \theta)\,\mathrm{d}\theta. \tag{64}$$

In the simplified expressions for unidirectional seas corresponding to (25)–(27) and (35)–(39) only the frequency spectrum appears. In the numerical calculations the integrands are expressed in terms of frequencies ω and ω' by the dispersion relation (54).

Double integrals $\int_\omega \int_{\omega'} \ldots \tilde{S}(\omega)\,\tilde{S}(\omega')\,\mathrm{d}\omega\,\mathrm{d}\omega'$

were calculated using the very efficient iterative procedure described in the previous section.

Figures 4 and 5 show the observed probability distribution for the horizontal and vertical velocities for the different elevations. In the same figures the continuous parts of the density function given in (21) are presented leaving out the discrete part. The observed probability distribution for time series $\bar{u}_i$ and $\bar{w}_i$ are estimated and then scaled in the same manner as the surface elevation ζ_i (see (61)). The only difference is that the modified velocity values given in (60), which are equal to zero and correspond to $\zeta_i < z$, are not counted in the appropriate bin. For elevations $z = -0.05$ m and $z = 0$ m

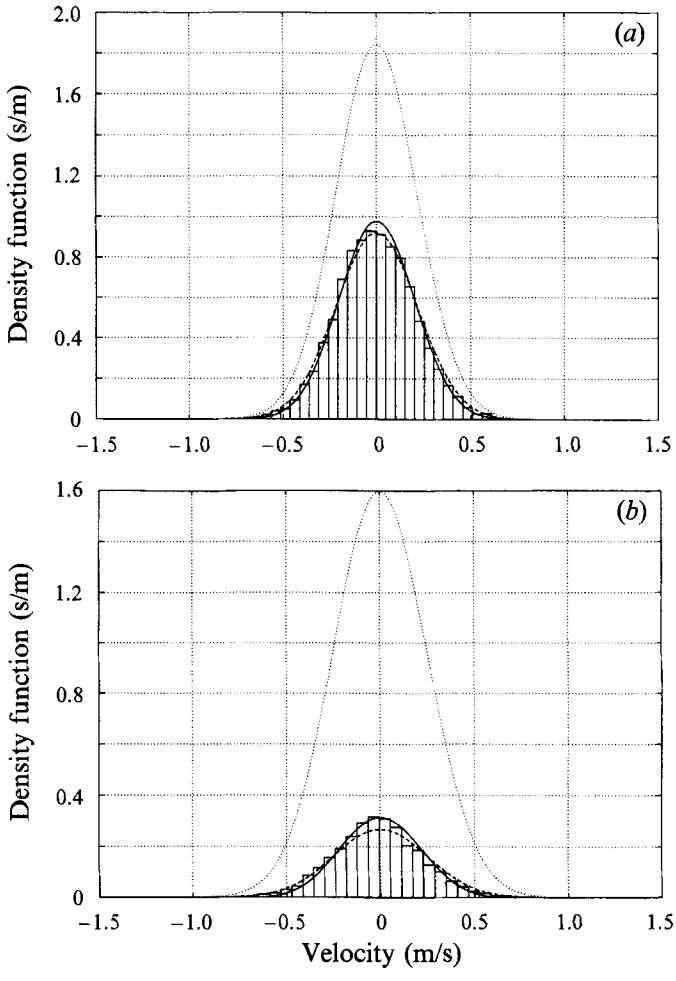

FIGURE 5. Continuous part of probability density function of the vertical velocity for various z: (*a*) Run 25, $z = 0$ m, (*b*) Run 10, $z = 0.05$ m. Bar plot, observed values; ——, second-order according to (15); – – –, first-order according to (21); · · · · ·, first-order without emergence effect (Gaussian).

the theoretical results (when the emergence effect is taken into account) are in close agreement with the observed values. When the measurement point of the LDV station is above the mean water level the agreement is slightly better when the nonlinearity of the wave motion is included, i.e. (15) compares better with the experimental data. For the lower position of the LDV station the differences due to weak second-order nonlinearities are marginal. However the emergence effect is still important for elevations $z > -3\sigma_\zeta$. In figures 4 and 5 the Gaussian probability density function is marked for comparison.

The density functions for the horizontal velocity component are generally skewed while those for the vertical velocity are unskewed.

Figures 6 and 7 show the variation of the mean value and standard deviation along the z-axis for the horizontal and vertical velocity, respectively. It can be noted that differences between theoretical values due to second-order nonlinear effects ((18) and (19)) and without these effects ((22) and (23)) are negligible. Only slightly better agreement for the standard deviation of the horizontal velocity in the second-order

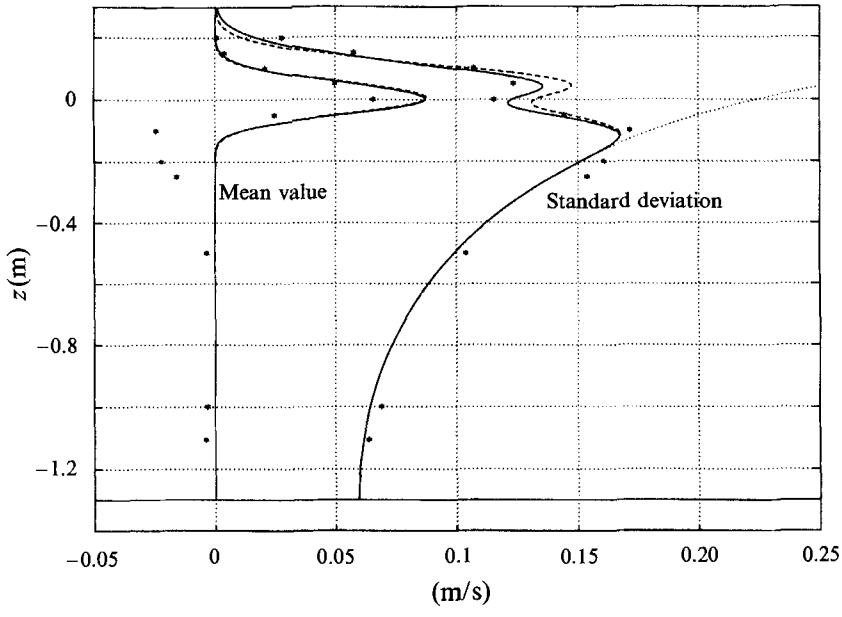

FIGURE 6. Mean value and standard deviation of horizontal velocity as functions of elevation z for wave case I18: *, observed values; ——, second-order; – – –, first order; · · · · ·, first-order without emergence effect taken into account.

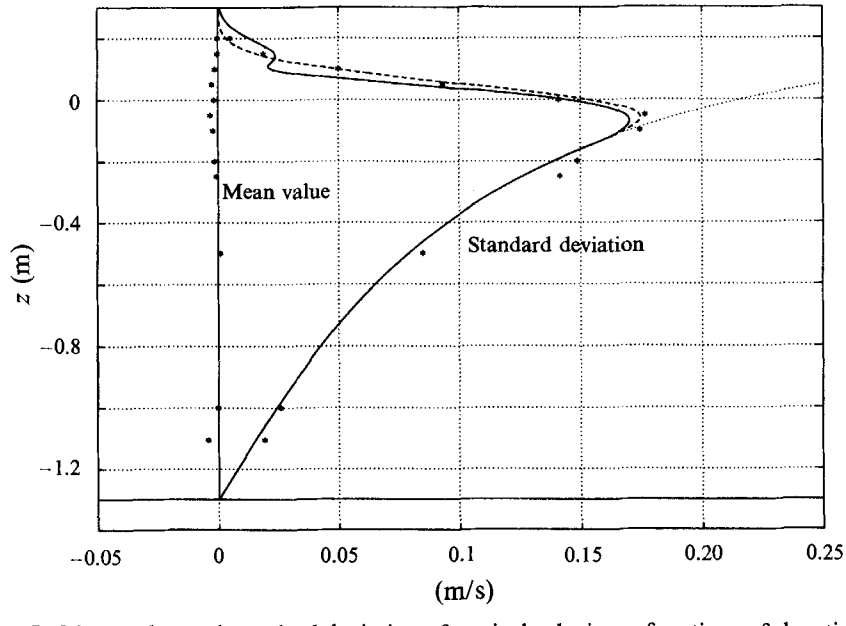

FIGURE 7. Mean value and standard deviation of vertical velocity as functions of elevation z for wave case I18: *, observed values; ——, second-order; – – –, first-order; · · · · ·, first-order without emergence effect taken into account.

approximation can be noticed. The observed values show a high degree of agreement with theoretical values obtained with the emergence effect taken into account and also compare well with the findings of Anastasiou *et al.* (1982*a*, *b*). However, for the mean value of the horizontal velocity, the observed values do not compare well with those

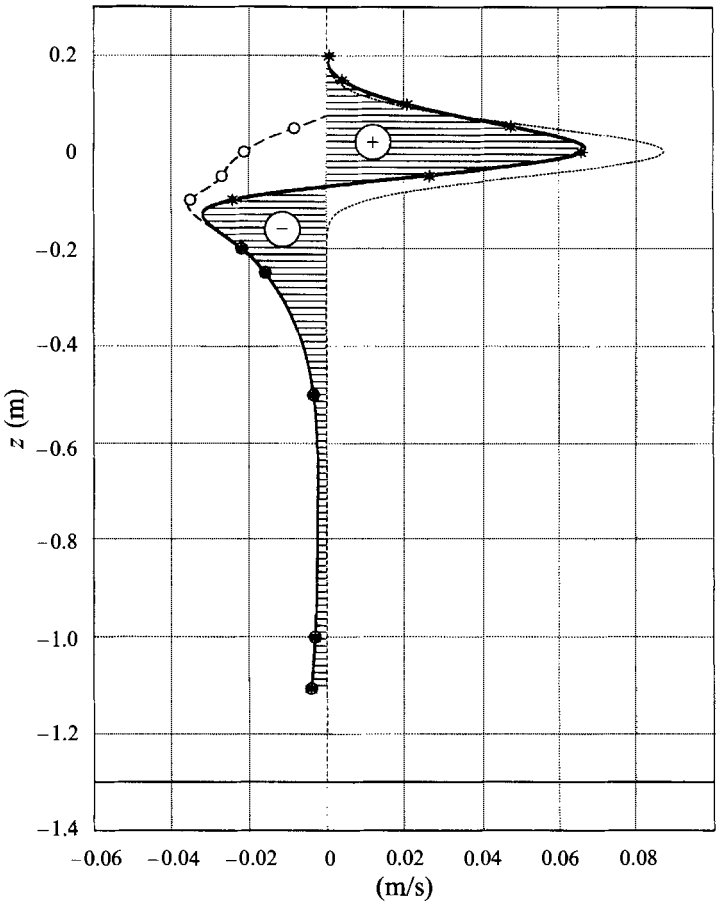

FIGURE 8. Mean value of horizontal velocity and estimate of return flow for wave case I18: *, observed mean values; ---, according to formula (22); ○, estimated return flow.

obtained theoretically. It seems that the existence of the return current in a confined wave flume could be an explanation of that departure. The emergence effect 'produces' a positive mean value of the horizontal velocity (an apparent current) in the vicinity of the mean water level. This current, directed along the positive x-axis, has to be balanced by the return current. In this way the measured values of the horizontal component of the particle velocity will be influenced by the backflow in the wave tank. In fact it should be stated that the theory presented in §2 for horizontal velocities cannot be verified from the data taken from a closed wave flume. These theoretical results may be valid only for waves in the open sea. Note that we are not able to introduce the simplest solution suggested for the return flow problem, i.e. the assumption of a uniform distribution. We operate in the domain $z \in [-h, \infty)$ and such an assumption would not have made sense.

However, we can rephrase the problem. If we believe that the results obtained in §2 are correct, then we can suggest that the difference between the predicted and the measured values gives an estimate of the return current in the wave flume! In figure 8 the measured mean horizontal velocities are marked with stars for wave case I18. The dashed line presents the theoretical mean value of the horizontal velocities with the emergence effect taken into account, according to (22). Open circles show the

Wave case	q^+ ($m^2 s^{-1}$)	Δq ($m^2 s^{-1}$)	χ	q_m^+ ($m^2 s^{-1}$)	Δq_m ($m^2 s^{-1}$)	χ_m
I18	0.0115	1.61×10^{-4}	0.014	0.0082	3.76×10^{-4}	0.047

TABLE 2. Numerical results for wave case I18.

estimated, as described above, values of the return flow. It should be emphasized that the only 'true' part of that figure are points for the measured and estimated velocities of the mean horizontal velocity and the estimated return flow, respectively, as well as the curve for the theoretical mean horizontal velocity. The solid lines for the measured mean velocity and the estimated return flow should be treated as 'intuitive guesses' for the appropriate vertical mean velocity profiles. They were obtained by use of cubic spline interpolation.

The interpolated profiles as well as the theoretical values for the positive mean value of the horizontal velocity were used to estimate the measured positive and negative total flows q_m^+, q_m^-, respectively, and the predicted positive total mean flow q^+, induced by the waves, and the estimated return flow q^-. Let us denote

$$\left.\begin{aligned} \chi_m^{\pm} &= \frac{\Delta q_m}{|q_m^{\pm}|}, \quad \chi_m = \tfrac{1}{2}(\chi_m^+ + \chi_m^-), \\ \chi^{\pm} &= \frac{\Delta q}{|q^{\pm}|}, \qquad \chi = \tfrac{1}{2}(\chi^+ + \chi^-), \end{aligned}\right\} \tag{65}$$

where $\Delta q_m = q_m^+ + q_m^-$ and $\Delta q = q^+ + q^-$. The value q^+ obtained from theoretical formula (51) for wave case I18 is presented in table 2. It denotes the positive total mean flux calculated by numerical integration with the spectrum $S(\omega)$ estimated from the time series ζ. Table 2 also shows the quantities Δq, Δq_m obtained from numerical computations together with the coefficients χ and χ_m. Note that the above values (except for q^+ which is calculated from the theoretical expression) are influenced by the authors' 'intuitive guess' expressed in artificial lines and that they should be treated as a rough estimation. Nevertheless, the numerical results obtained for χ, χ_m in (65) of order 5% (see table 2) indicate that the constraint of zero net mass flow seems to be fulfilled.

A zero mean value of the vertical velocity for all elevations follows from (18), (38) and (45). This agreed very well with observations, cf. figure 7.

Figure 9 shows the skewness of the horizontal velocity calculated with the help of (39) and (40) (when weak nonlinearities are taken into account). These values appear to be slightly negative, which is in close agreement with measured skewness at elevations deeply below the mean water level where the emergence effect is not important. Anastasiou *et al.* (1982*b*) also noted the negative skewness values for horizontal velocity. Owing to the emergence effect the skewness becomes positive close to the mean water level, cf. figure 9. The theoretical predictions for the skewness of the horizontal velocity with the emergence effect taken into account (for cases with and without second-order nonlinear effects) are also presented in figure 9. They were obtained by numerical integration of the probability density (15) and compare well with the observed skewness.

The skewness of the vertical velocity, for points below the mean water level, is zero in accordance with (43). This is confirmed in figure 9 where the calculated skewness of the measured vertical velocities is marked with open circles.

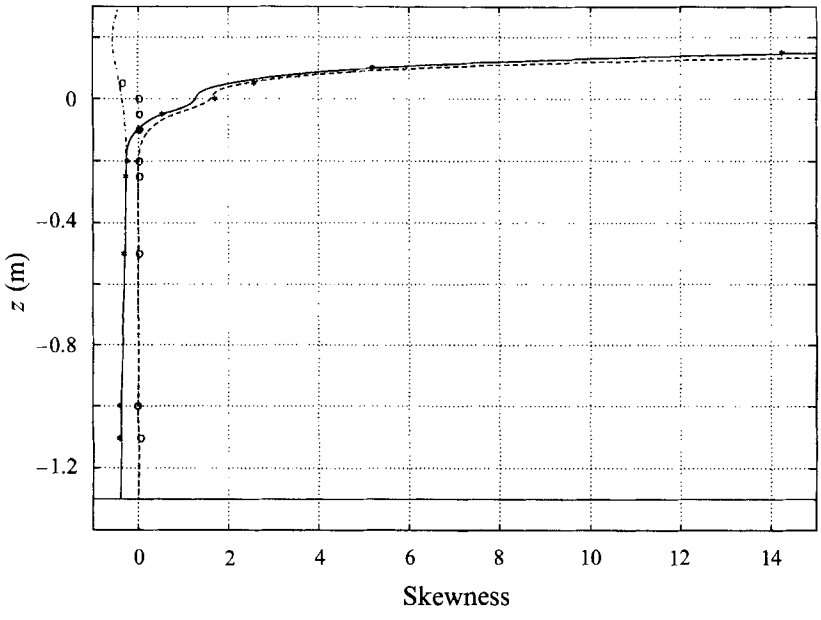

FIGURE 9. Skewness of particle velocity as function of elevation z for wave case I18. Horizontal: ——, second-order; – – –, first-order; ·–·–·–, second-order without emergence effect taken into account; *, observed values. ○, vertical observed values.

4. Conclusions

It is proposed that the values of a stationary and homogeneous nonlinear random process can be expressed as a series of random functions while the upper boundary for which the process has physical values is expressed as another series of random variables. Through this proposal the expressions for general random fields can be applied to the process. Defining the modified water wave velocities of a wave field as the kinematics below the surface of the waves and zero above the surface, the theory and expressions for random fields can then be applied to water wave kinematics.

Starting from the basic equations of hydrodynamics, the statistical properties of wave kinematics can be expressed in terms of the linear part of the surface elevation spectrum and there is no need to make assumptions regarding the analytical expressions for the wave kinematics. It should be noted that this allows the prediction of the statistics of wave kinematics knowing only the parameters or the data that are required to establish the wave surface elevation spectrum.

Following the development of the theoretical predictions, wave surface and wave kinematics measurements are analysed, with particular emphasis on the near-surface kinematics. For the wave case I18 generated from an almost linear wave surface spectrum, it is demonstrated that nonlinearities have a marginal effect on the measured kinematics and that non-Gaussian parts of the statistics of wave kinematics mainly relate to the emergence effects. For a sea state generated from a more strongly nonlinear surface spectrum it is, however, expected that the effects on the kinematics from the surface nonlinearities would have been significant.

Excellent correlation between the statistical measurements and predicted theoretical results has been found, thus demonstrating the usefulness of this theoretical development, the only difference found between predictions and measurements being that for the mean value of the horizontal velocity near the free surface.

An attempt is made in this paper to demonstrate that the non-zero mean horizontal velocity (in the Eulerian frame) resulting from taking into account the emergence effect should be treated as a mass transport velocity. This is done by showing that the formulae obtained for the total mean flux in approximation lead to the known and well-interpreted formulae for mass flux usually obtained in the Lagrangian frame.

An alternative method for derivation of the mean water flux in the region near the mean water level is presented. The relevant formulae are developed in the Eulerian frame for random water waves. The approximate value of the total mean flux is previously known (Phillips 1960) but the approach presented in this paper is in the authors' opinion more direct in the sense that only the definition of the total mean flux and the expression for the horizontal particle velocity are needed. Moreover, traditional approaches allow us only to treat the total flux like a physical quantity 'existing on a subset of zero measure', namely, exactly on the free surface of the wave. Within such an approach we are not able, in the Eulerian frame, to discuss the distribution of the mean velocity in the free-surface zone. We would then have the situation that the mean velocity along the vertical is everywhere equal to zero except at the free surface. In the present approach the mean velocity is 'stretched out' from the exact location of the surface onto the free-surface zone. More precisely, for the random wave case, theoretically a non-zero mean horizontal velocity should exist from $z = -h$ to infinity (due to the Gaussian distribution for free surface elevation, this zone should, however, in practice be treated as the region near the mean water level). Moreover, we are able to calculate not only the total mean water flux but also the flux between two given z-elevations.

The theoretical results of this study, when applied to horizontal velocities, are valid only in open water. It follows that these results cannot be directly verified with measurements taken in a wave tank. However, if we postulate that these theoretical results are correct, then we can suggest that the difference between the predicted and the measured values gives an estimate of the return current in the wave flume. Postulating that the formulae obtained in this paper are correct is supported by two factors:

(i) that the expression for the total mean flux in approximation is known and well-interpreted, as was mentioned above;

(ii) that the approach for estimating such stochastic properties of random water wave kinematics, which are not influenced by the return flow (i.e. mean value of the vertical velocity and standard deviation for both horizontal and vertical velocity components) agrees very well with the measurements in the wave flume.

Experimentalists do not normally study kinematics in the free-surface zone. This is mainly due to technical difficulties associated with data collection in this zone. The measurements usually have been stopped at an elevation where interesting phenomenon just appear. The first measurements of wave kinematics near the mean water level (up to one standard deviation of the surface elevation above that level) were reported by Anastasiou *et al.* (1982*a*, *b*). The data set which has been examined in this paper is, however, unique in the sense that it has been possible to examine the variation of the velocity along the vertical axis up to a level of about four standard deviations of the surface elevation and down to the bottom of the wave flume with measurements spaced close enough to prepare the profiles for the statistical properties of the velocities.

Reviewing the I18 wave case, currents in opposite directions to each other have been noticed. While the emergence effect explains the existence of a current in the direction of wave advance, the nature of the return current which appears just below the mean water level is still unresolved (at least for irregular waves). To answer the question why

this layer is 'preferred' by the backflowing water, it may be necessary to take into account the viscosity of the fluid in the near-boundary regions and the vorticity which diffuses and convects throughout the wave flume. Energy dissipation and the turbulence in the free-surface zone may be also important factors which influence the shape of the mean horizontal velocity profile. For a complete study of the problem of the return flow in a flume, the full three-dimensional geometry and details of wave absorption need to be considered.

Further work will concentrate on evaluation of other data series to examine the influence of wave steepness on wave kinematics and on further prediction of return flow in a wave flume.

The authors would like to thank Dr J. Skjelbreia and Professor A. Tørum for their efforts in providing the unique data material which has made verification of the theoretical prediction possible. This data collection was funded by the Norwegian Council for Scientific and Industrial Research, Statoil, Amoco, Conoco, Exxon and Mobil. Furthermore, the first author would like to express thanks to Professor S. Massel for his continuous support during preparation of the theoretical procedures presented in §2. The authors would also like to express thanks to the reviewers for helpful suggestions to improve the paper.

Appendix A

The probability density function for the modified random process $\bar{Y}(z)$ can be evaluated by the theorem of total probability (Tung 1975):

$$f_{\bar{Y}}(y) = f_{\bar{Y}|X<z}(y)\,P[X<z] + f_{\bar{Y}|X\geqslant z}(y)\,P[X\geqslant z], \tag{A 1}$$

where $f_{\bar{Y}|X<z}(y) = \delta(y)$ and

$$f_{\bar{Y}|X\geqslant z}(y) = \int_z^\infty f_{XY}(x,y)\,\mathrm{d}x / P[X\geqslant z]. \tag{A 2}$$

The joint density $f_{XY}(x,y;z)$ in the second-order approximation is provided by Longuet-Higgins (1963) as

$$f_{XY}(x,y;z) = \frac{1}{\sigma_X\,\sigma_Y(z)\,[\Delta(z)]^{\frac{1}{2}}} Z(y')\,Z(\eta)\,[1+\tfrac{1}{6}(\lambda_{30}\,H_{30}+3\lambda_{21}(z)\,H_{21} + 3\lambda_{12}(z)\,H_{12}+\lambda_{03}\,H_{03})], \tag{A 3}$$

where $\eta = \eta(x',y';r) = (x'-ry')/\Delta^{\frac{1}{2}}$ and $H_{mn} = H_{mn}(x',y';r)$.

Calculation of the conditional density in (A 2) reduces to evaluation of the following integrals:

$$\int_{x=z}^{+\infty} H_{mn}(x',y';r)\,Z(y')\,Z[\eta(x',y';r)]\,\mathrm{d}x. \tag{A 4}$$

There are two kinds of such integrals – when $m \geqslant 1$ and when $m = 0$. In the first case we obtain

$$\begin{aligned}\int_{x=z}^{+\infty} & H_{mn}(x',y';r)\,Z(y')\,Z[\eta(x',y';r)]\,\mathrm{d}x \\ &= -\frac{\sigma_X}{2\pi}\int_{x'=z'}^{+\infty}\frac{\partial}{\partial x'}[H_{m-1n}(x',y';r)\,\mathrm{e}^{-[y'^2+\eta^2(x',y';r)]/2}]\,\mathrm{d}x' \\ &= \sigma_X\,H_{m-1n}(z',y';r)\,Z(y')\,Z[\eta(z',y';r)].\end{aligned} \tag{A 5}$$

In the case $m = 0$ we can write

$$\int_{x=z}^{+\infty} H_{0n}(x', y'; r)\, Z(y')\, Z[\eta(x', y'; r)]\, \mathrm{d}x$$

$$= \sum_{k=0}^{n} \binom{n}{k} H_{n-k}(y')\, Z(y') \int_{x=z}^{+\infty} (-1)^k \frac{\partial^k}{\partial y'^k} Z[\eta(x', y'; r)]\, \mathrm{d}x$$

$$= \sigma_X \Delta^{\frac{1}{2}} \Big\{ H_n(y')\, Z(y')\, Q[\eta(z', y'; r)]$$

$$- \frac{1}{(2\pi)^{\frac{1}{2}}} Z(y') \sum_{k=1}^{n} (-1)^k \binom{n}{k} \left(\frac{r}{\Delta^{\frac{1}{2}}}\right)^k H_{n-k}(y')$$

$$\times \int_{\gamma=\eta(z', y'; r)}^{+\infty} \frac{\partial}{\partial \gamma} \left[(-1)^{k-1} \frac{\partial^{k-1}}{\partial \gamma^{k-1}} \mathrm{e}^{-\gamma^2/2} \right] \mathrm{d}\gamma \Big\}, \tag{A 6}$$

and then, by (11), one can obtain the following expression for the integral:

$$\int_{x=z}^{+\infty} H_{0n}(x', y'; r)\, Z(y')\, Z[\eta(x', y'; r)]\, \mathrm{d}x = \sigma_X \Delta^{\frac{1}{2}} Z(y') \Big\{ H_n(y')\, Q[\eta(z', y'; r)]$$

$$+ Z[\eta(z', y'; r)] \sum_{k=1}^{n} (-1)^k \binom{n}{k} \left(\frac{r}{\Delta^{\frac{1}{2}}}\right)^k H_{n-k}(y')\, H_{k-1}[\eta(z', y'; r)] \Big\}, \tag{A 7}$$

in which $H_0(x) = 1$.

Equation (A 3), through (A 5) and (A 7) (where by (12) $P[X < z] = 1 - Q^*(z')$), leads to the probability density for $\bar{Y}(z)$ in the form of (15).

In order to calculate the first two statistical moments of the modified process $\bar{Y}(z)$, the values of the following integrals

$$I_{mn}^k = \int_{-\infty}^{+\infty} y^k \int_{x=z'}^{+\infty} H_{mn}(x, y; r)\, Z(y)\, Z[\eta(x, y; r)]\, \mathrm{d}x\, \mathrm{d}y \tag{A 8}$$

for $k = 1, 2$ and $m+n \leqslant 3$ should be known. Integration by parts results in

$$I_{mn}^1 = 0 \quad \text{for} \quad n \geqslant 2 \quad \text{and} \quad I_{mn}^2 = 0 \quad \text{for} \quad n \geqslant 3. \tag{A 9}$$

Successive integrals are given as

$$I_{30}^1 = \int_{-\infty}^{+\infty} y H_{20}(z', y; r)\, Z(y)\, Z[\eta(z', y; r)]\, \mathrm{d}y$$

$$= \frac{\partial^2}{\partial z'^2} \left\{ Z(z') \int_{-\infty}^{+\infty} y Z[\eta(y, z'; r)]\, \mathrm{d}y \right\} = r \Delta^{\frac{1}{2}} H_3(z')\, Z(z'), \tag{A 10}$$

where the following relation was used:

$$Z(y)\, Z[\eta(x, y; r)] = Z(x)\, Z[\eta(y, x; r)]. \tag{A 11}$$

Furthermore

$$I_{21}^1 = -\int_{-\infty}^{+\infty} y \frac{\partial}{\partial y} \{ H_{10}(z', y; r)\, Z(y)\, Z[\eta(z', y; r)] \}\, \mathrm{d}y. \tag{A 12}$$

Integrating by parts, using (A 11) leads to

$$I_{21}^1 = -\frac{\partial}{\partial z'} \left\{ Z(z') \int_{-\infty}^{+\infty} Z[\eta(y, z'; r)]\, \mathrm{d}y \right\} = \Delta^{\frac{1}{2}} H_1(z')\, Z(z'). \tag{A 13}$$

Since
$$\frac{\partial}{\partial y} Q[\eta(z', y; r)] = \frac{r}{\Delta^{\frac{1}{2}}} Z[\eta(z', y; r)] \tag{A 14}$$

we have
$$I^1_{00} = -\Delta^{\frac{1}{2}} \int_{-\infty}^{+\infty} \left(\frac{\partial}{\partial y} Z(y)\right) Q[\eta(z', y; r)]\, \mathrm{d}y = r\Delta^{\frac{1}{2}} Z(z'). \tag{A 15}$$

Successive integrals for $k = 2$ can be obtained in the same manner. Their values are

$$\left.\begin{aligned} I^2_{00} &= \Delta^{\frac{1}{2}}[Q^*(z') + r^2 H_1(z')\, Z(z')], \quad & I^2_{30} &= \Delta^{\frac{1}{2}} H_4(z')\, Z(z'), \\ I^2_{21} &= 2\Delta^{\frac{1}{2}} r\, H_2(z')\, Z(z'), & I^2_{12} &= 2\Delta^{\frac{1}{2}} Z(z'), \end{aligned}\right\} \tag{A 16}$$

Appendix B

As mentioned in §2.1, the random field of the free surface elevation $\zeta(\boldsymbol{x}, t)$ may be represented by (3). For this stationary and homogeneous random field there exists, on the other hand, the following Stieltjes–Fourier representation:

$$\zeta(\boldsymbol{x}, t) = \int_{\boldsymbol{k}} \mathrm{d}A(\boldsymbol{k}) \exp[\mathrm{i}(\boldsymbol{k}\cdot\boldsymbol{x} - \omega t)], \tag{B 1}$$

in which $\mathrm{d}A(\boldsymbol{k})$ is a complex random field. The representation given by (B 1) allows one to define the continuous spectral density $F(\boldsymbol{k})$ by

$$\langle \mathrm{d}A(\boldsymbol{k})\, \mathrm{d}A^*(\boldsymbol{k}')\rangle = F(\boldsymbol{k})\, \delta(\boldsymbol{k} - \boldsymbol{k}')\, \mathrm{d}\boldsymbol{k}\, \mathrm{d}\boldsymbol{k}' \tag{B 2}$$

where an asterisk denotes complex conjugate.

The spectrum $F(\boldsymbol{k})$ contains energy associated with both the first and the higher-order, forced components (see Tick 1959). Thus we can write

$$F(\boldsymbol{k}) = F^{(1)}(\boldsymbol{k}) + F^{(2)}(\boldsymbol{k}) + \ldots, \tag{B 3}$$

where $F^{(1)}(\boldsymbol{k})$ and $F^{(2)}(\boldsymbol{k})$ are the first- and second-order parts of the spectrum $F(\boldsymbol{k})$, respectively.

For the free-surface displacement ζ, the random variables ξ_i in (3), for say, $i = 1, \ldots, N = 2N'$ are specified according to Longuet-Higgins (1963) such that

(i) ξ_i can be divided into two groups: $i = 1, \ldots, N'$ and $i = N'+1, \ldots, N$,

(ii) their variances $V_i = \langle \xi_i^2 \rangle$ are

$$V_i = \frac{1}{2}\begin{cases} \langle a_i^2 \rangle & \text{for} \quad i = 1, \ldots, N' \\ \langle a_{i-N'}^2 \rangle & \text{for} \quad i = N'+1, \ldots, N, \end{cases} \tag{B 4}$$

where a_i, $i = 1, \ldots, N'$, associated with wavenumber $\boldsymbol{k}_i$, are the first-order amplitudes of ζ.

According to Longuet-Higgins (1963), the relation between the variances V_i and the spectral density $F(\boldsymbol{k})$ is such that when $N \to \infty$ each $V_i \to 0$ in such a way that

$$F^{(1)}(\boldsymbol{k})\, \mathrm{d}\boldsymbol{k} = \sum_{\substack{\boldsymbol{k}_i \in \mathrm{d}\boldsymbol{k} \\ i \in \{1, \ldots, N'\}}} V_i = \sum_{\substack{\boldsymbol{k}_i \in \mathrm{d}\boldsymbol{k} \\ i \in \{N'+1, \ldots, N\}}} V_i \tag{B 5}$$

over any small but fixed region in the $\boldsymbol{k}$-plane. This means that when $N \to \infty$ (and $N' \to \infty$)

$$\int_{\boldsymbol{k}} F^{(1)}(\boldsymbol{k})\, \mathrm{d}\boldsymbol{k} = \sum_{i=1}^{N'} V_i = \sum_{i=N'+1}^{N} V_i. \tag{B 6}$$

Where series $\sum_i \dots V_i$, appear, one can then obtain integrals by

$$\sum_{i=1}^{N'} \dots V_i, \quad \sum_{i=N'+1}^{N} \dots V_i \underset{\text{or } N\to\infty}{\overset{N'\to\infty}{\to}} \int_k \dots F^{(1)}(\boldsymbol{k})\,\mathrm{d}\boldsymbol{k}. \tag{B 7}$$

The first three statistical moments of the random variable X will hereafter be discussed. It can be shown that these moments can be expressed in terms of V_i as follows:

$$\begin{aligned} m_1 &= \sum_{i=1}^{N} \alpha_{ii} V_i + \dots, \\ \mu_2 &= \sum_{i=1}^{N} \alpha_i \alpha_i V_i + 2 \sum_{i,j=1}^{N} \alpha_{ij} \alpha_{ij} V_i V_j + \dots, \\ \mu_3 &= 6 \sum_{i,j=1}^{N} \alpha_i \alpha_j \alpha_{ij} V_i V_j + \dots . \end{aligned} \tag{B 8}$$

In a first-order approximation one obtains

$$m_1 = 0, \quad \mu_2 = \sum_{i=1}^{N} \alpha_i \alpha_i V_i, \quad \mu_3 = 0. \tag{B 9}$$

In the next approximation due to Longuet-Higgins (1963)

$$m_1 = \sum_{i=1}^{N} \alpha_{ii} V_i, \quad \mu_2 = \sum_{i=1}^{N} \alpha_i \alpha_i V_i, \quad \mu_3 = 6 \sum_{i,j=1}^{N} \alpha_i \alpha_j \alpha_{ij} V_i V_j, \tag{B 10}$$

which means that, in this approximation, terms of order V^2 can be neglected when compared with terms which are of order V.

By the assumption of stationarity and homogeneity one can in the case when X is specified as the free-surface elevation consider the special point $\boldsymbol{x} = \boldsymbol{0}$ and time $t = 0$. For this case Longuet-Higgins (1963) has shown that

$$\alpha_i = \begin{cases} 1 & \text{for} \quad i = 1, \dots, N' \\ 0 & \text{for} \quad i = N'+1, \dots, N. \end{cases} \tag{B 11}$$

Thus, in view of (B 10) and (B 7) at second order

$$\mu_2 = \sum_{i=1}^{N'} V_i = \int_k F^{(1)}(\boldsymbol{k})\,\mathrm{d}\boldsymbol{k} \tag{B 12}$$

when $N' \to \infty$.

On the other hand, it is obvious that $\mu_2 = \int_k F(\boldsymbol{k})\,\mathrm{d}\boldsymbol{k}$, which means that the difference between the true value of the variance μ_2 and the calculated value as given by (B 12), in view of (B 8) is of order

$$\int_k F^{(2)}(\boldsymbol{k})\,\mathrm{d}\boldsymbol{k} = \sum_{i,j=1}^{N'} \Omega_{ij} V_i V_j, \tag{B 13}$$

where Ω_{ij} is a certain constant associated with the pair of wavenumber vectors $(\boldsymbol{k}_i, \boldsymbol{k}_j)$. In order to obtain the parameters of the probability distribution given by (15) (which are primarily given in the form of series $\sum_i \dots V_i$, $\sum_{i,j} \dots V_i V_j$), (B 7) demonstrates that the linear part of the spectrum $F^{(1)}(\boldsymbol{k})$ must be known. In the authors' opinion, however, there is no need to split the spectrum into its first- and second-order parts for practical calculations. Within the assumed accuracy, the linear part of the spectrum

can be approximated by the full spectrum. This is consistent with Longuet-Higgins' (1963) second-order approximation given by (B 10) but contrary to Anastasiou *et al.* (1982*b*). In fact, under such an assumption (i.e. using $F(\boldsymbol{k})$ instead of $F^{(1)}(\boldsymbol{k})$), the first two statistical moments, which are of order V, are obtained with an error of order V^2 (while for the free-surface elevation ζ the 'ideal' variance is obtained), and third moments, being of order V^2, are calculated with an error of order V^4.

REFERENCES

ANASTASIOU, K., TICKELL, R. G. & CHAPLIN, J. R. 1982*a* Measurements of particle velocities in laboratory-scale random waves. *Coastal Engng* **6**, 233–254.

ANASTASIOU, K., TICKELL, R. G. & CHAPLIN, J. R. 1982*b* The non-linear properties of random wave kinematics. In *BOSS 82 – Proc. Third Intl Conf. on the Behaviour of Offshore Structures*, vol. 1, pp. 493–515. Hemisphere.

CIEŚLIKIEWICZ, W. 1985 Nonlinear approach to the problem of probability distributions of the orbital velocities and pressures for wind-induced waves. *Arch. Hydrot.* **32**, 192–220 (in Polish).

CIEŚLIKIEWICZ, W. 1989 Stochastic characteristics of wind waves in the vicinity of still water level. PhD thesis, Institute of Hydroengineering, Gdańsk, Poland (in Polish).

CIEŚLIKIEWICZ, W. & MASSEL, S. R. 1988 Interaction of wind waves with vertical wall. *J. Waterway, Port, Coastal Ocean Engng ASCE* **114**, 653–672.

GUDMESTAD, O. T. 1990 A new approach for estimating of irregular deep water wave kinematics. *Appl. Ocean Res.* **10**, 19–24.

ISAACSON, M. & BALDWIN, J. 1990 Random wave forces near free surface. *J. Waterway, Port, Coastal Ocean Engng ASCE* **116**, 232–251.

LONGUET-HIGGINS, M. S. 1963 The effect of non-linearities on statistical distributions in the theory of sea waves. *J. Fluid Mech.* **17**, 459–480.

OCHI, M. K. & WANG, W. C. 1984 Non-gaussian characteristics of coastal waves. In *Proc. 19th Coastal Eng. Conf.* vol. 1, pp. 516–531. ASCE.

OPPENHEIM, A. V. & SCHAFER, R. W. 1975 *Digital Signal Processing*. Prentice Hall.

PAJOUHI, K. & TUNG, C. C. 1975 Statistics of random wave field. *J. Waterways, Harbors Coastal Engng Div. ASCE* **101** (WW4), 435–449.

PHILLIPS, O. M. 1960 The mean horizontal momentum and surface velocity of finite-amplitude random gravity waves. *J. Geophys. Res.* **65**, 3473–3476.

PHILLIPS, O. M. 1977 *The Dynamics of the Upper Ocean*, 2nd edn. Cambridge University Press.

SARPKAYA, T. & ISAACSON, M. 1981 *Mechanics of Wave Forces on Offshore Structures*. Van Nostrand Reinhold.

SKJELBREIA, J. E., BEREK, E., BOLEN, Z. K., GUDMESTAD, O. T., HEIDEMAN, J. C., OHMART, R. D., SPIDSØE, N. & TØRUM, A. 1991 Wave kinematics in irregular waves. In *Proc. 10th Intl Conf. on Offshore Mechanics and Arctic Engng*, pp. 223–228. ASME.

SKJELBREIA, J., TØRUM, A., BEREK, E., GUDMESTAD, O. T., HEIDEMAN, J. & SPIDSØE, N. 1989 Laboratory measurements of regular and irregular wave kinematics. In *E & P Forum Workshop on Wave and Current Kinematics and Loading IFP, Rueil Malmaison, France, E & P Forum Rep.* 3.12/156, pp. 45–66.

TICK, L. J. 1959 A non-linear random model of gravity waves. *J. Math. Mech.* **8**, 643–652.

TØRUM, A. & GUDMESTAD, O. T. 1990 (Ed.) *Water Wave Kinematics*. NATO ASI, Series E: Applied Sciences, vol. 178. Kluwer.

TUNG, C. C. 1975 Statistical properties of the kinematics and dynamics of a random gravity wave field. *J. Fluid Mech.* **70**, 251–255.

WHEELER, J. D. 1970 Method for calculating forces produced by irregular waves. *J. Petrol. Tech.* **3**, 359–367.

ZELT, J. A. & SKJELBREIA, J. E. 1992 Estimating incident and reflected wave fields using an arbitrary number of wave gauges. *Proc. 23th Coastal Engng Conf., Venice, Italy* (in press).